Journal of Theoretical Biology 419 (2017) 77–89

Contents lists available at ScienceDirect

Journal of Theoretical Biology

journal homepage: www.elsevier.com/locate/yjtbi

Temperature cycles affect colonization potential of calanoid copepods

Harshana Rajakaruna[a,*], Mark Lewis[b,c]

[a] Mathematical Biology Unit, Okinawa Institute of Science and Technology Graduate University, Japan
[b] Centre for Mathematical Biology, Department of Biological Sciences, University of Alberta, Canada
[c] Department of Mathematical and Statistical Sciences, University of Alberta, Canada

ARTICLE INFO

Keywords:
Population fitness
Net reproductive rate
Intrinsic growth rate
Invasive species
Periodic temperature fluctuations

ABSTRACT

Marine calanoid copepods colonize new habitats, and some become invasive. Their fitness, measured by intrinsic growth rate and net reproductive rate, is partially driven by biochemical processes. Thus, it is a function of ambient temperature. Biochemical processes may not be approximated well by yearly mean temperature alone when temperature cycles yearly, largely. Higher order moments may also be important. The amplitude of yearly fluctuations of monthly and seasonal sea temperatures varies dramatically across the northern temperate regions. Thus, they can impact the fitness, thereby the colonization potential of copepods migrating across such region. To investigate this, we derive approximate metrics of periodic (yearly) fitness: the *yearly intrinsic growth rate*, and a *weighted net reproductive rate*. We use them to measure the persistence and the growth of an Allee-effect free, stage-structured, fast-maturing, small population of invasive copepods that reproduces year-round in habitats with yearly temperature cycles. We show that the *yearly fitness* increases substantially when a population is introduced from a habitat with large amplitude to that with small amplitude yearly fluctuating temperatures, given that their mean temperatures and other environmental and ecological factors are constant. The detected range-expansion of the modeled species matches the potential fitness gradient predicted by the metrics. The study leads to the question whether the gradient of the amplitudes of temperature between habitats with similar yearly mean temperatures impacts a class of fast-maturating calanoid copepods, colonizing new habitats, and becoming invasive.

1. Introduction

Marine copepods colonize new habitats across and along the coasts via human mediated vectors such as ship ballastwater discharge (e.g., Cordell et al., 2009; Boltovskoy et al., 2011) and natural vectors such as ocean currents (Damerau et al., 2012; Gillespie et al., 2012). Human mediated introductions have accelerated the colonization and invasion rates (Hulme, 2009; Lockwood et al., 2013), which have potentially led to changed ecosystem structures, risking ecosystem functions. Ruiz et al. (2011) have discussed the impacts of non-indigenous marine and estuary copepods introduced to North America. As copepods are a major link between primary and tertiary producers in large marine food webs, in which humans are an end-receiver (Kiørboe, 2008), there is an escalating concern regarding which environmental and ecological processes and factors enhance the colonization potential and the invasibility of copepods in order to manage human-mediated colonization (see Bollens et al. (2012)).

It has been shown that life-history traits, such as fecundity, mortality and maturation rates, of copepods are functions of ambient temperature (Uye et al., 1983; Kiorboe and Sabatini, 1994; 1995; Liang and Uye, 1997a, 1997b; Kiorboe and Hirst, 2008). For ectotherms, in general, Amarasekare and Savage (2011) have shown that ambient temperature can impact fitness, measured by intrinsic growth rate λ, which is governed by biochemical processes, whereas Strasser et al. (2011) have shown a case specific to invasive calanoid copepod *Eurytemora affinis*. Rajakaruna et al. (2012) also have shown that temperatures can determine the potential and the limits to persistence, growth, and geographic distribution of invasive marine calanoid copepod *Pseudodiaptomus marinus,* with respect to their net reproductive rate R_O, modeled explicitly as a function of ambient temperature. Yet, all these models implicitly assume that average ambient temperature of a habitat is a good approximation to the full system, while other environmental and ecological factors are assumed to be constants.

Typically, sea surface temperature (SST) is considered as the ambient temperature of copepods dwelling in the upper ocean habitats. The monthly mean SSTs fluctuate periodically (yearly) at varying amplitudes, as large as 15 °C, in northern temperate regions (data

* Corresponding author.
E-mail addresses: harshana.rajakaruna@dfo-mpo.gc.ca (H. Rajakaruna), mark.lewis@ualberta.ca (M. Lewis).

http://dx.doi.org/10.1016/j.jtbi.2017.01.044
Received 12 April 2016; Received in revised form 24 January 2017; Accepted 31 January 2017
Available online 08 February 2017
0022-5193/ © 2017 Elsevier Ltd. All rights reserved.

from NOAA-ESRL (n.d.)). When temperature fluctuates largely, Savage (2004) has shown that measuring the rate of change of biochemical processes on the basis of average temperature is a weak approximation, thus, incorporating second-order responses are also important. Therefore, he concluded that one must be extremely cautious as to which geographic locations one applies such models, as temperature fluctuates largely in some temperate regions. In line with the theory for ectotherms by Savage (2004), the fluctuations of sea temperature can impact the fitness of copepods dwelling in the upper ocean habitats, thus, their colonization potential and geographic distribution. Therefore, both λ and $R_{O,}$ calibrated with respect to yearly mean habitat temperatures, can be insufficient to understand the full system dynamics of copepod populations in habitats with yearly temperature cycles. Therefore, to study the impact of the degree (amplitude) of yearly temperature cycles on fitness, and thereby, persistence, growth and colonization potential of copepods, we need new metrics of fitness, measured across the yearly temperature cycles, as opposed to that assume constant temperature environments.

To test the impact of temperature fluctuations on copepod fitness, we study the year-round reproducing invasive marine calanoid copepod *P marinus,* native to Japan, colonizing marine and estuary habitats around the world (Uye et al., 1983; Rajakaruna et al., 2012; Brylinski et al., 2012; Jha et al., 2013; Sabia et al., 2015). A class of marine calanoid copepods has a similar stage-structure (Mauchline and Mauchline, 1998), and qualitatively similar functional responses of vital rates, such as, fecundity, mortality (Hirst and Kiørboe, 2002; Bunker and Hirst, 2004), and generation times (Huntley and Lopez, 1992) to temperature.

The aim of our study is to understand the effect of the amplitude of yearly (periodically) fluctuating temperatures, or yearly temperature cycles, at monthly and seasonal scales, on fitness, and thus, the colonization potential of a small, but Allee effect free, population of the model-species *P marinus* introduced to new habitats, and thereby, to predict their potential geographic distribution, isolating temperature. To investigate this, we derive metrics that determine the persistence (stability) and the growth of a population, approximating fitness, in yearly temperature cycles. Here, we choose *P. marinus* for deriving the metrics, because functional dependencies of its vital rate parameters on temperature, and geographical distribution and colonization histories, are recorded well in the literature.

2. Model

2.1. Life-history and population dynamics of P.marinus

Copepod *Pseudodiaptomus marinus,* reproduces year-round, resulting overlapping generations, has 13 life-history stages; eggs, 6 nauplier, 5 copepodite stages, and a reproducing adult stage; with first nauplier stage commonly disregarded for computations as it lasts only for few seconds (Uye et al., 1983; Liang and Uye, 1997a, 1997b). This results in 12 effective stages for our computations. Their stage-structure is common for a large class of marine calanoid copepods (Mauchline and Mauchline, 1998).

A general form of a linear, continuous time (t day), population growth that depends on periodic (yearly) ambient temperature T (°C) can be written as a system of ODE,

$$\frac{d\mathbf{n}}{dt} = \mathbf{A}[T(t)]\mathbf{n} \tag{1}$$

where $\mathbf{n}$ is a vector of the stage-composition of abundances (number), and $\boldsymbol{A}(T(t))$ is the transition matrix with time-periodic coefficients with period t_P (year). All notations are given in Table 1. Although Eq. (1) is a linear system of dimension $\mathbf{n}$, the entries in the transition matrix $\mathbf{A}$ are non-linear functions of temperature T (°C) and T is a non-linear function of time t (day), and hence entries in $\mathbf{A}$ are non-linear functions of time t. The system is called *invasible* if the $\mathbf{n}=\mathbf{0}$ equilibrium solution is unstable, and hence the ecological invasibility condition translates into a mathematical stability condition for the system in Eq. (1). Here, we intend to study the stability and constraint-free (intrinsic) growth of a small, but an Allee-effect free population.

The coefficients of the transition matrix $\mathbf{A}\in\Re^{lxl}$ of *P. marinus* are functions of ambient temperature $T(t)$ (°C) (Rajakaruna et al., 2012), with lxl dimensions. Stage-maturation times (days) of copepods are Gamma distributed, of which, the shape parameter k, which mechanizes the stage-developmental delays, can be approximated by the integer 3 for copepods, in general (Read and Ashford, 1968; Breteler et al., 1994), including for *P. marinus* (Rajakaruna et al., 2012). As parameter k in Gamma distributed stage-maturation times is equivalent to k virtual sub-stages within each stage in the matrix $\mathbf{A}(T)$, consistent with the theory of linear chain trick in ordinary differential equation (ODE) systems (Cox, 1967), $\mathbf{A}(T)$ can be written with 3 sub-stages within each stage for *P. marinus* (see life-history diagram in Appendix [A]). It gives,

$$\mathbf{A}(T) = \begin{pmatrix} -\sigma_1(T) & & & & \vdots & & & q\beta_s(T) & q\beta_s(T) & q\beta_s(T) \\ \gamma_1(T) & -\sigma_1(T) & & & \vdots & & & & & \\ & \gamma_1(T) & -\sigma_1(T) & & \vdots & & & & & \\ & & \gamma_1(T) & -\sigma_2(T) & \vdots & & & & & \\ \vdots & \vdots & \vdots & \vdots & \vdots & \vdots & \vdots & \vdots & \vdots & \vdots \\ & & & & \vdots & -\sigma_{s-1}(T) & & & & \\ & & & & \vdots & \gamma_{s-1}(T) & -\sigma_s(T) & & & \\ & & & & \vdots & & \gamma_s(T) & -\sigma_s(T) & & \\ & & & & \vdots & & & \gamma_s(T) & -\mu_s(T) & \end{pmatrix}.$$

Here, μ_i and γ_i are stage-dependent mortality and maturation rate parameters (per day), respectively, for each 3 sub-stages in stage i. Similarly, parameter $\sigma_i = \mu_i + \gamma_i$ is the total removal rate (per day) of individuals from each sub-stage, and β_s is the average number of eggs produced by a female (per day) in adult stage s. The proportion of ovigerous females in the adult population, q, is approximately 0.61 for *P. marinus* (Liang and Uye, 1997a, 1997b). Thus, $l=sk$, where s is the number of stages, 12, and k is the number of virtual sub-stages, 3, in each stage i. Note that this system is dynamically equivalent to a slightly simpler version (see Appendix [B]) with $l=k(s-1)-1$.

We use the quadratic function $\mu = \kappa_0 + \kappa_1 T + \kappa_2 T^2$ to model mortality rates, assuming μ is a concave up function, with high mortality at both high and low temperatures for *P. marinus* (as in Rajakaruna et al. (2012)). Here, κ_0, κ_1 and κ_2 are parameters. Rajakaruna et al. (2012) also showed that μ is stage-independent, as confidence intervals, given by the model fitted to distinct stages, overlap with one another. The Arrhenius function, which assumes mortality rate of ectothermic species, in general, is exponentially decreasing with decreasing temperature (Gillooly et al., 2001; Savage et al., 2004; Amarasekare and Savage, 2011), can also be numerically approximated by a quadratic function. Hirst and Kiørboe (2002) show that mortality rate data of copepod species, tested at different temperatures, fit to such functional forms well.

We use the Gaussian function $\beta_s = b_0 \exp[-(T - b_1)^2/b_2]$ to model fecundity rate, which is a generic form for ectothermic species (Amarasekare and Savage, 2011). Here, b_O, b_1 and b_2 are parameters. This function has the flexibility to fit to fecundity data at any range of temperatures: increasing (e.g., copepods in tropical and subtropical waters), or decreasing (e.g. copepods in cold waters), or increasing and decreasing (copepods in temperate waters), with increasing temperature (see the patterns of fecundity data in Uye (1981), Sullivan and McManus (1986), Saiz et al. (1999), Halsband-Lenk et al. (2002), Gislason (2005), Holste and Peck (2006) and Kang et al., 2011). The generalized exponentially increasing trend, shown in fecundity rate data, pooled from a large collection of copepod species experiments, by Hirst and Kiørboe (2002) and Bunker and Hirst (2004), may turn Gaussian, had the species been modeled separately (i.e., if species effect is statistically accounted) and tested within a full range of sea

Table 1
Notations and equations.

Notation	Description
$\mathbf{n}$	Vector of stage-abundance composition (numbers).
t	Time (day).
T	Ambient temperature (°C).
$\mathbf{A}$	Transition matrix with time-periodic coefficients .
k	Number of sub-stages in each stage i; k=3 for *P. marinus*.
s	Number of stages (12 for *P. marinus* after sub-stage N1 is dropped).
l	Dimensions of matrix $\mathbf{A}$; l=sk; also, l=$k(s-1)-1$ in the reduced matrix (see Appendix [B]).
j	Denotes the time interval ($t_{jd} - t_{(j-1)d}$), where d is the number of days in the interval; for e.g., if the interval j is a month, for j=1..m, s.t., m=12, then d=30 days (approx.); and if the interval j is a season in a two-season year, then m=2, and d=180.5 days (approx.) if seasons are time-symmetric.
$\mathbf{A_j}$	Transition matrix of time interval j (month or season), assuming temperature T_j of the intervals are constants.
i	Denotes any sub-stage of stage i.
t_P	Period (year): $t_p = \sum_{j=1}^{m}(t_{jd} - t_{(j-1)d}) = t_{md} - t_0$ (days), where t_{md} is the end time, and t_O is the initial time of the period.
μ_i	Sub-stage mortality rate (per day) of stage i. Model generalized for all stages: $\mu = \kappa_0 + \kappa_1 T + \kappa_2 T^2$, where κ_0, κ_1 and κ_2 are parameters.
γ_i	Sub-stage maturation rate (per day) of stage i: $\gamma_i = (T-1)^b/(\alpha_i - \alpha_{i-1})$, where α_i for i=0:13 with $\alpha_0 = 0$ are temperature–independent coefficients and parameter b=1.8 for *P. marinus*.
$\sigma_i = \mu_i + \gamma_i$	Total removal rate of individuals (per day) from a sub-stage of stage i.
β_s	Average number of eggs produced by a female (per day) in adult stage s: $\beta_s = b_0 \exp(-(T-b_1)^2/b_2)$, where b_O, b_1 and b_2 are parameters.
q	Proportion of ovigerous females in the adult population.
$(\lambda_j, \mathbf{v}_j)$	Dominant eigen-pair of $\mathbf{A}_j$ for j=1..m: λ_j is the intrinsic growth rate (number per interval j) at constant temperature T_j; and $\mathbf{v}_j$ is the eigenvector corresponds to the eigenvalue λ_j.
$\mathbf{n}(t_0)$	Vector of stage-abundance composition (numbers) at initial time t_O; $\mathbf{n}(t_0)$=$N_0\mathbf{v_0}$, where N_0 is the initial population abundance; s.t., N_0=$\|\|\mathbf{n}(t_0)\|\|$.
N_m	Population abundance at interval j=m; N_m=$\|\|\mathbf{n}(t_m)\|\|$; where m is the last interval of the year (period).
V	A measure of the time-averaged variation in the stage-structure through the year: $V = (1/t_p)\sum_{j=1}^{m}\log(\mathbf{v}_{j-1}, \mathbf{v}_j) \leq 0$.
$\bar{\lambda}$	Time-averaged piecewise intrinsic growth rates (number per interval): $\bar{\lambda} = (1/t_p)\sum_{j=1}^{m}\lambda_j(t_{jd} - t_{(j-1)d})$.
g_j	Mean sub-stage removal time (days) in interval j (month or season). That is, the average of $1/\sigma_i$ of the sub-stages of stage i in interval j, where $\sigma_i = \mu_i + \gamma_i$ for each sub-stage in stage i, except for the last sub-stage in last stage $k(s-1)+1$, where $\sigma_i = \mu_i$.
P_j	Proportion of the number of sub-stages removed within the interval j (month or season) at constant temperature T_j, to the total number of sub-stages removed within the whole year: $P_j = \left(\frac{t_{jd} - t_{(j-1)d}}{g_j}\right) / \sum_{j=1}^{m}\left(\frac{t_{jd} - t_{(j-1)d}}{g_j}\right)$;
$R_{0,j}$	Net reproductive rate (number) at interval j (month or season) corresponds to constant temperature T_j: $R_{0,j} = \frac{q\beta_{s,j}}{\mu_j}\prod_{i=1}^{s-1}\left(\frac{\gamma_{i,j}}{\gamma_{i,j}+\mu_j}\right)^k$;
g_p	Average sub-stage removal time (days) of the population over the year (period): $g_p = t_p / \sum_{j=1}^{m}\left(\frac{t_{jd} - t_{(j-1)d}}{g_j}\right)$;
R_p	Weighted periodic (yearly) net reproductive rate (number per year): $R_p = \left(\sum_{j=1}^{m} P_j R_{0,j}^{\left(\frac{1}{l}\right)} + g_p V\right)^l$. Here, l=k(s-1)+1.
Λ_p	An approximation to the maximal Lyapunov (Floquet) exponent (number per year): $\Lambda_p = \bar{\lambda} + V$, also written as $\Lambda_p = \frac{1}{g_p}\left(R_p^{\frac{1}{l}} - 1\right)$, where l=k(s-1)+1.
T_j	Temperature (°C) at intervals j: $T_j = B_0 + B_1 \sin(2\pi t/t_p + B_2)$; where B_O, B_1 and B_2 are parameters.

temperatures from approximately −2 °C to 34 °C. The logistic type functional form used by Rajakaruna et al. (2012), which assumes a ceiling in fecundity rate at higher temperatures, also fit well to the data of *P. marinus*.

The maturation rates of *P. marinus* are given by the Belehradek's function, $\gamma_i = (T-1)^b/(\alpha_i - \alpha_{i-1})$, where, α_i for i=0:13 are temperature–independent coefficients, with $\alpha_0 = 0$, and b=1.8 (Uye et al., 1983). The maturation rate at each sub-stage in stage i is given by $k\gamma_i(T)$, and thus, the maturation time of stage i is given by $1/\gamma_i(T)$ (Rajakaruna et al., 2012). Generation times of copepods with respect to temperature can be generalized for copepods (Huntley and Lopez, 1992), so can be their inverse functions, yielding the development rates.

2.2. Derivation of metrics of periodic fitness

Eq. (1) cannot be solved explicitly for many forms of $\mathbf{A}(T(t))$, which is referred to as the "great matrix exponential tragedy" (Moler and van Loan, 2003), including the one for *P. marinus*. However, when the coefficient matrix $\mathbf{A}(T(t))$ is periodic in time, Floquet theory can be used to show that there exists a unique solution to the initial value problem (Barone et al., 1977; Klausmeier, 2008). This solution has an associated fundamental matrix; the monodromy matrix; which is unique and time-invariant, and whose exponents can be used to determine the stability and growth of the system (Wang and Hale, 2001). Alternative methods of solutions assume piecewise constant $\mathbf{A}(T(t))$ with time discretized over the period into intervals (e.g., Gökçek, 2004), and also analytical approximations (e.g., Moler and van Loan, 2003). In essence, all these methods agree with Floquet theory, and are efforts to transform the non-autonomous system into an autonomous system. Yet, they do not give explicit solutions that can be written in the form of a fitness-metric, as a function of meaningful temperature-dependent vital rate parameters of our interest. The above solutions can be different from those given by $\mathbf{A}(T(t))$, when $T(t)$ is replaced by the average temperature of the period, assuming temperature fluctuations are negligible. As in Rajakaruna et al. (2012), such an assumption leads Eq. (1) to have an explicit analytic solution. Time-averaging of coefficients of $\mathbf{A}(T(t))$ also gives the stability condition, but not the rate of growth of the system (Ma and Ma, 2006; Wesley and Allen, 2009).

We solve Eq. (1) by piece-wise constant approximation. By doing so, we assume that quantitative responses of stage-based fecundity, mortality, and maturation rates of a population to change of temperature are approximated best at a scale longer than instantaneous. As generation times of *P. marinus* are weeks, approximately 23 days at 20°C, while average stage-removal times (for maturation plus mortality) are days (Uye et al., 1983; Rajakaruna et al., 2012), we assume that discretization of time by month or longer is a reasonable scale for the vital rates to yield quantitative responses to the respective changes in

temperature. Discretization of time by intervals, as large as months, for *P. marinus* is also justified on an empirical basis, as vital rate parameters, which we used for predicting their geographic distribution, have been estimated with the data from populations tested at different constant temperatures over time, but at changing temperatures (Uye et al., 1983; Rajakaruna et al., 2012).

We assume that $\mathbf{A}(T(t))$ can be approximated by constant matrices $\mathbf{A}_j$, for j=1,..,m, such that j corresponds to the interval $(t_{jd}\text{-}t_{(j-1)d})$, where d is the number of days of the interval, t_O is the initial time, and t_{md} is the end time of a period (year=md days). This assumption is on the basis that the system in mean temperature T_j, at interval j, for j=1,..m, is sufficiently long enough so as to allow the population to achieve a stable-stage distribution within that interval, as characterized by the eigen function associated with the dominant eigenvalue of $\mathbf{A}_j$. Note that, for example, m=12 in the case of time discretized by months j; for j=1..12, over a year, such that d is approximately 30 days, and m=2 in the case of time discretized by two seasons j; for j=1,2, over a year, such that d is approximately 182.5 days assuming time-symmetry. As monthly mean sea temperatures have smooth transitions from one month to another across the period, we assume that change of stable-stage distributions of *P. marinus* also may follow smooth transitions without drastic changes in response to change in monthly mean temperatures.

We denote the starting stage-abundance distribution by $\mathbf{n}(t_O)$ (numbers) at time t_O (day) of an year. Thus, based on Eq. (1), we can write the population at the end of the given year, with period t_P, as,

$$\mathbf{n}(t_p + t_0) = \mathbf{n}(t_{md}) = \left(\prod_{j=1}^{m} \exp((t_{jd} - t_{(j-1)d})\mathbf{A}_j)\right)\mathbf{n}(t_0), \tag{2}$$

where *exp* denotes the matrix exponentiation, and $t_p = \sum_{j=1}^{m}(t_{jd} - t_{(j-1)d}) = t_{md} - t_0$ (days). The Lefkovitch matrix $\mathbf{A}_j$ has a complete set of eigenvectors and a dominant eigenvalue with a corresponding eigenvector that has non-negative entries (Lefkovitch, 1965). If the intervals $(t_{jd}\text{-}t_{(j-1)d})$'s are spaced sufficiently, such that one or more generations are produced during the interval, which can be a month or a season in our calibrations, then it is reasonable to assume that $\mathbf{n}(t_{jd}) = \exp((t_{jd} - t_{(j-1)d})\mathbf{A}_j)\mathbf{n}(t_{(j-1)d}) \approx (\mathbf{n}(t_{(j-1)d}), \mathbf{v}_j)\exp(\lambda_j(t_{jd} - t_{(j-1)d}))\mathbf{v}_j$. Here, $(\mathbf{a},\mathbf{b})$ denotes the dot product of vectors $\mathbf{a}$ and $\mathbf{b}$, and $(\lambda_j, \mathbf{v}_j)$ is the dominant eigen-pair of $\mathbf{A}_j$ for j=1..m. Each eigenvector is normalized such that $(\mathbf{v}_j,\mathbf{v}_j)$=1. The above assumption is justified for *P. marinus*, as we will see that their sub-stage generation times are generally shorter than a month in our estimations (Uye et al., 1983; Rajakaruna et al., 2012). Applying the above recursively from t_O to t_{md} yields $\mathbf{n}(t_{md}) = N_0(\mathbf{v}_0, \mathbf{v}_1)\ldots(\mathbf{v}_{m-1}, \mathbf{v}_m)\mathbf{v}_m \exp\sum_{j=1}^{m}\lambda_j(t_{jd} - t_{(j-1)d}) = N_{md}\mathbf{v}_m$. Here, $\mathbf{v_O}$ describes the initial composition of the population, so that, $\mathbf{n}(t_0)=N_0\mathbf{v_O}$, where $N_0=||\mathbf{n}(t_0)||$. Here, $N_{\mathrm{md}}=||\mathbf{n}(t_{\mathrm{md}})||$, and $\mathbf{n}(t_{\mathrm{md}}) = N_{\mathrm{md}}\mathbf{v_m}$. Taking the inner product of this equation with $\mathbf{v_m}$ yields $N_{md} = N_0(\mathbf{v}_0, \mathbf{v}_1)\ldots(\mathbf{v}_{m-1}, \mathbf{v}_m)\exp\sum_{j=1}^{m}\lambda_j(t_{jd} - t_{(j-1)d})$, where $N_{\mathrm{md}}=(\mathbf{n}(t_{\mathrm{md}}),\mathbf{v}_{\mathrm{m}})$, and $N_0=(\mathbf{n}(t_0),\mathbf{v}_0)$. Hence, we can define the average growth rate (number) per period (year), $\Lambda_p = (1/t_p)\log(N_{md}/N_0)$, as

$$\Lambda_p = \bar{\lambda} + V \tag{3}$$

where, $\bar{\lambda} = (1/t_p)\sum_{j=1}^{m}\lambda_j(t_{jd} - t_{(j-1)d})$ is the time-averaged piecewise intrinsic growth rates, λ (number per interval; month or season), and, $V = (1/t_p)\sum_{j=1}^{m}\log(\mathbf{v}_{j-1}, \mathbf{v}_j)$, which is ≤0, is a measure (number) of the time-averaged variation in the stage-structure through the year. The Λ_p gives an approximation to the maximal Lyapunov (Floquet) exponent. Therefore, in general, we can write an approximate condition for population persistence in this periodic system as $\Lambda_p > 0$. Thus, Λ_p can be interpreted as an approximate *yearly* (*periodic*) *intrinsic growth rate* of the population, or the *yearly fitness* parameter of the population in a yearly fluctuating temperature environment. The λ, given by the average temperature of the year, is a special case of Λ_p, as Λ_p approximates λ when amplitude tends to zero.

To analyze the conditions by which Λ_p holds true, biologically, and for further biological insights into temperature-time profile driven colonization dynamics, we derive a *weighted yearly* (*periodic*) *net reproductive rate* R_p (number per year), based on Λ_p (Eq. [3]), given by

$$R_p = \left(\sum_{j=1}^{m} P_j R_{0,j}^{\left(\frac{1}{l}\right)} + g_p V\right)^l, \tag{4}$$

such that, $\Lambda_p = (1/g_p)\left(R_p^{\frac{1}{l}} - 1\right)$ for a population in a habitat with periodically fluctuating temperature (see Appendix [C] for derivation). Here, $P_j = \left(\frac{t_{jd} - t_{(j-1)d}}{g_j}\right) / \sum_{j=1}^{m}\left(\frac{t_{jd} - t_{(j-1)d}}{g_j}\right)$ is the proportion of the number of sub-stages removed within the interval j, i.e., $(t_{jd} - t_{(j-1)d})$, which can be for e.g., a month or a season, at constant (or mean) temperature T_j of the interval, to the total number of sub-stages removed within the year. Here g_j is the mean sub-stage removal time in interval j, that is, the average of $1/\sigma_i$ of the sub-stages in interval j, where $\sigma_i = \mu_i + \gamma_i$ for each sub-stage in stage i, except for the last sub-stage in last stage $k(s-1)+1$, where $\sigma_i = \mu_i$. Here, $l=k(s\text{-}1)+1$, $R_{0,j} = \frac{q\beta_{s,j}}{\mu_j}\prod_{i=1}^{s-1}\left(\frac{\gamma_{i,j}}{\gamma_{i,j}+\mu_j}\right)^k$ is the net reproductive rate over the interval j associated with matrix $\mathbf{A_j}$, and g_p is the average sub-stage removal time of the population over the year (period), that is, $g_p = t_p / \sum_{j=1}^{m}\left(\frac{t_{jd} - t_{(j-1)d}}{g_j}\right)$. Population persists if $R_p > 1$, following $\Lambda_p > 0$.

Although there is no computational advantage of using R_p over Λ_p, in general, when V=0, as was the case for *P. marinus*, $R_p = \left(\sum_{j=1}^{m} P_j R_{0,j}^{\left(\frac{1}{l}\right)}\right)^l$, which is an explicit function of temperature-dependent biological parameters μ, γ_i and β_s at given piece-wise constant (or mean) temperatures (T_j) of intervals j, month or a season, over the period (year). The R_p can be interpreted as the number of offspring at an end of a periodic cycle, through generations of females starting from an ovigerous female at the begging of the cycle. The R_O, given by the average temperature of the year, is a special case of R_p, as R_p approximates R_O when amplitude tends to zero. Here, P_j can be used to analyze the effect of time-asymmetric periodic fluctuations of temperature also, and in any scales of time-discretization, on R_p, as long as they are biologically justified. It gives that the general condition for R_p, and therefore, Λ_p, to exist in a biologically meaningful way, is $g_j < (t_{jd}, t_{(j-1)d})$. The smaller the average stage-removal time (g_j) compared to the length which the population is in interval j, i.e., $(t_{jd}, t_{(j-1)d})$, the better is the approximation as a general theory. This also suggests that for species having longer g_j require lager discretized intervals for both R_p and Λ_p to make sense.

Furthermore, for e.g., for a simple case, in which for a population to persist a periodic two-season environment (m=2); one favorable ($R_{0,1} > 1$) and the other unfavorable ($R_{0,2} < 1$); it follows from R_p (for V=0) that $(R_{0,1}^{\left(\frac{1}{l}\right)} - 1)P_1 > (1 - R_{0,2}^{\left(\frac{1}{l}\right)})P_2$, that the product of the geometric mean of R_O per stage above 1 individual, and the average number of stages removed in the favorable season, should be greater than the product of the geometric mean of R_O per stage below 1 individual, and the average number of stages removed in the unfavorable season. Fig. 1 shows the theoretical basis of the reduction in $\Lambda_p(V = 0)$ with respect to an increase in the amplitude of two-season periodic temperatures on the basis of Jensen's (1906) inequality. This reduction is generally true for both $\Lambda_p(V = 0)$ and $R_p(V = 0)$ if λ is a concave function of temperature T.

3. Calibrations, test of approximations, and results

3.1. Calibration of parameters

We parameterized fecundity and mortality rate functions for *P. marinus* by data reconstructed from Liang and Uye (1997a) and

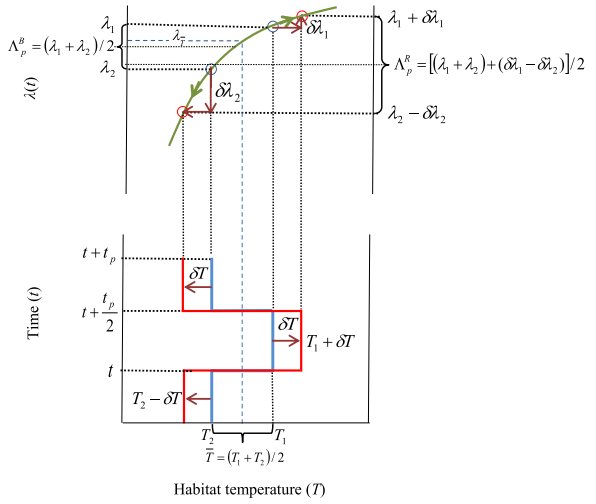

Fig. 1. The effect of increased amplitude of temperature on periodic intrinsic growth rate Λ_p (V=0) from Eq. (3). Green curve indicates $\lambda(T)$, the intrinsic population growth rate, which is a concave function of constant habitat temperatures $T(t)$. Here,λ_1 and λ_2 correspond to piecewise constant temperatures T_1 and T_2, respectively, of two seasons of the period t_p, of temperature-time function (B: blue curve). We increase amplitude by δT (R: red curve), while holding the mean habitat temperature the same. Arrows indicate the direction of change of $\lambda(T)$ w.r.t. increase in temperature amplitude by δT. Here, blue temperature profile yields $\Lambda_p^B = (\lambda_1 + \lambda_2)/2$ and the red temperature profile yields $\Lambda_p^R = (\lambda_1 + \delta\lambda_1 + \lambda_2 - \delta\lambda_2)/2$, resulting $\Lambda_p^R = \Lambda_p^B + (\delta\lambda_1 - \delta\lambda_2)/2$. As $\delta\lambda_2 > \delta\lambda_1$ due to concavity of $\lambda(T)$, we get $\Lambda_p^R < \Lambda_p^B$. Furthermore, $\Lambda_p^B < \lambda_{\bar{T}}$, similarly. These show that the higher the amplitude of periodic fluctuations, the lower is the Λ_p. The above result, which is due to Jensen's inequality, holds true, universally across $T(t)$, in general, if $\lambda(T)$ is a concave function of T. The above results w.r.t. R_p vs. R_o also behave similarly as we show that they are both functionally related to $\lambda(T)$.

Rajakaruna et al. (2012), respectively, minimizing the sum of squared residuals using *fminsearch* (MLE) procedure in Matlab. The Gaussian fecundity rate function, transformed from the statistical model in (Fig. 2A), is given by $\beta_s = 13.6\exp[-(T - 22.51)^2/80.33]$ with R^2 =0.96. The quadratic mortality rate function is given by $\mu = 0.508 - 0.067T + 0.0025T^2$ with R^2=0.64 (Fig. [2B]). We used the maturation rate model $\gamma_i = 3(T - 1)^{1.8}/(\alpha_i - \alpha_{i-1})$, estimated for *P. marinus* for sub-stages of stage i, where α_i values were [55.01, 134.21, 325.81, 557.4, 864.01, 1110.77, 1479.68, 1827.22, 2159.64, 2656.81, 3353.02, 4321.76] for i=1..12, and $\alpha_0 = 0$, from Rajakaruna et al. (2012) (Fig. [2C]). These compartmental models allowed us to calculate the matrix $\mathbf{A}_j$ for any given piecewise constant temperatures T_j at months j, for j=1..12. The data of *P. marinus* come from both laboratory and field experiments, conducted at different fixed temperatures (see Rajakaruna et al. (2012) for details).

3.2. Test of approximations

To investigate model-approximations empirically, and predict potentially invasible habitats of *P. marinus*, we used long-term monthly mean sea surface temperature (SST) data from 1971 to 2000 at $1^0\times1^0$ latitudinal and longitudinal resolution via satellite from NOAA-ESRL (n.d.). For 100 randomly selected $1^0\times1^0$ resolution marine plots, we computed Λ_p (for $V\neq0$) from Eq. (3) via (λ_j, $\mathbf{v}_j$) using Matlab function *eig()* based on parameterized $\mathbf{A}_j$ for SST data at monthly intervals j, for j=1..12. This Λ_p is numerically equivalent to the maximal Lyapunov (Floquet) exponent given by *log(max(real(eig(expm(A_1) expm(A_2).. expm(A_{12})))))/12* in Matlab following Gökçek (2004). We compared Λ_p (for $V\neq0$), statistically, with maximal Lyapunov (Floquet) exponent Λ_p computed via monodromy matrix, **M**, for **A** in Eq. (1), denoted by Λ_p(M), for the same data, using Runge-Kutta scheme 2 given by Wang and Hale (2001) at 0.01 day intervals, as per their recommendation. This is to test the effect of scale of discretization of Λ_p , given that in both cases the responses of vital rates to temperature were modeled at the scale of monthly mean temperatures. The metric Λ_p(M) is given by *log(max(real(eig(M))))/12* in Matlab. (Fig. 3A) shows the differences (in Ai) and the correlation (in Aii) between Λ_p from Eq. (3) for $V\neq0$, and $\Lambda_p(M)$ computed via monodromy matrix from long-term monthly mean SST data of 100 randomly selected $1^0\times1^0$ marine plots. The high R^2 and gradient close to 1 suggest that the difference between the two metrics is negligible. Therefore, the computation of Λ_p using Eq. (3), with time discretized at monthly intervals, versus the standard maximal Floquet exponent computed via monodromy matrix, with time discretized at 0.01 day, has no empirical difference, given that in both cases the quantitative response of parameters to temperatures are modeled at monthly mean temperature scale.

We compared Λ_p (for V=0), statistically, with Λ_p (for $V\neq0$) for the same SST data to investigate if V=0 assumption in the derivation of simplified R_p as a function of biologically explicit parameters from Eq. (4). The function Λ_p (for V=0) is given by *sum[max-(real(eig(A_1)))+max(real(eig(A_2)))+...+max(real(eig(A_{12})))]/12* in Matlab. (Fig. 3B) shows the differences (in Bi) and the correlation (in Bii) between Λ_p from Eq. (3) for $V\neq0$, and Λ_p for V=0 for the same SST

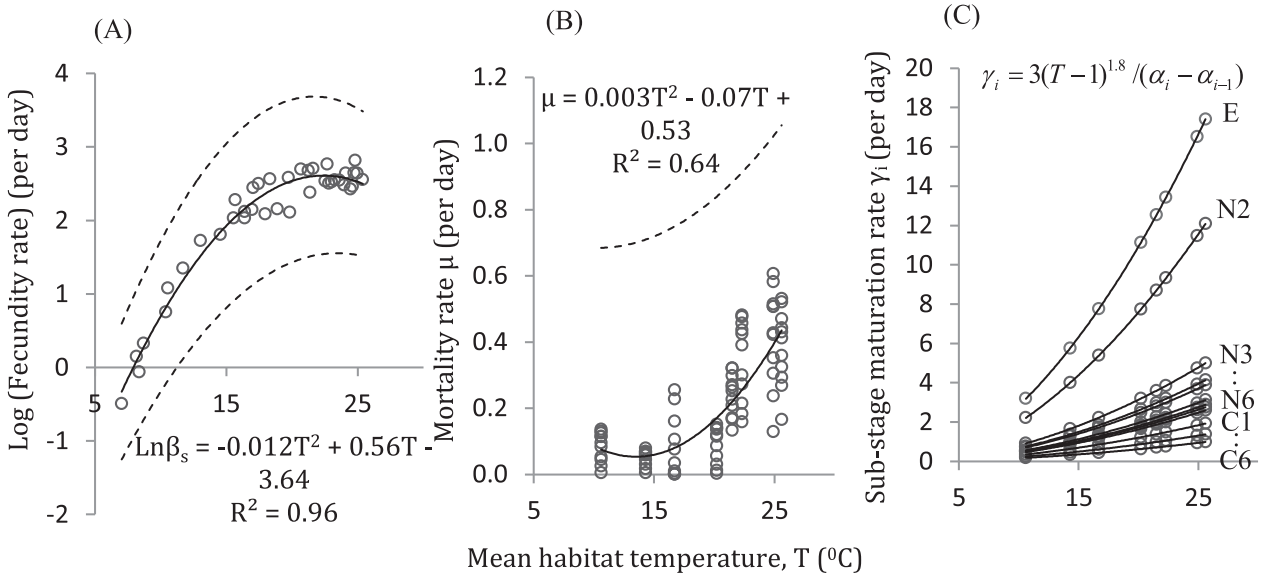

Fig. 2. (A) Statistical model of log-fecundity rate per day, (B) mortality rate per day, and (C) sub-stage maturation rate (per day), based on α_i values estimated by Rajakaruna et al. (2012). Here, stages i=1..12 are E-eggs, N2,N3.. N6–naupli, C1.. C6–copepodite (C6-female adults), respectively. Dashed lines are 95% CI.

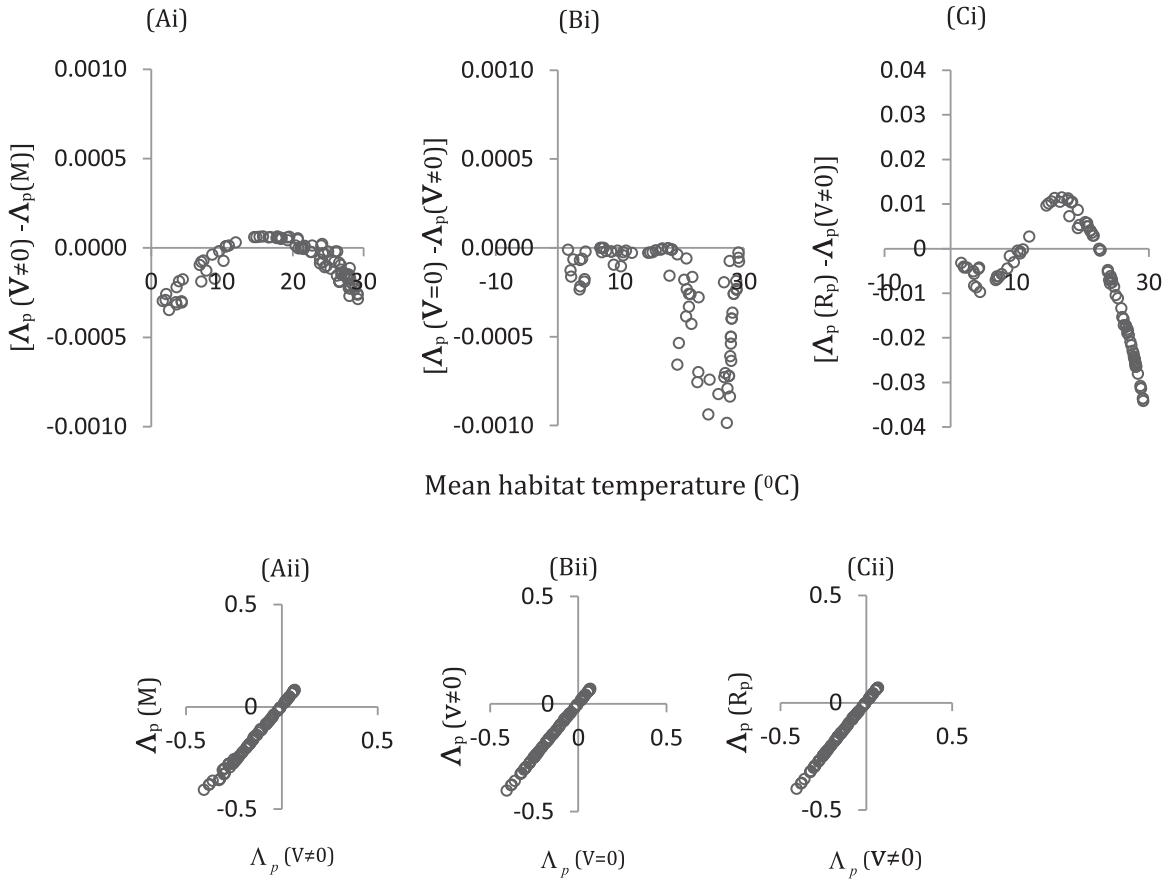

Fig. 3. (Ai) Difference between Λ_p (V≠0) from Eq. (3) and Λ_p (via M: Monodromy Matrix) estimated by long-term monthly mean SST of 100 random $1^0 \times 1^0$ marine plots from NOAA-ESRL (n.d.). (Bi) Difference between Λ_p (V=0) and Λ_p (V≠0) both from Eq. (3) estimated for the same SST data. (Ci) Difference between Λ_p (via R_p) from Eq. (4) with V=0, and Λ_p (V≠0) from Eq. (3) estimated for the same SST data. (Aii, Bii, Cii) All regressions yielded R^2=0.99 and gradient=1.0.

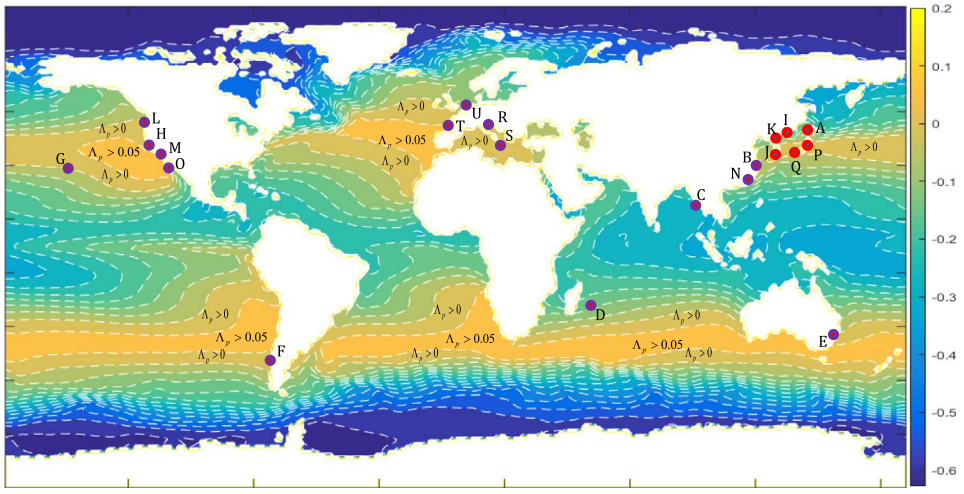

Fig. 4. Yearly intrinsic growth rate Λ_p, given by the colour scheme, estimated for *P. marinus*, based on long-term monthly mean SST data at $1^0 \times 1^0$ spatial resolution from NOAA-ESRL (n.d.). Red circles show habitats, which *P. marinus* are native to (Walter, 1986) –surrounding the Sea of Japan. Purple circles are habitats where *P. marinus* was detected (Olazabal and Tirelli, 2011; Brylinski et al., 2012; Jha et al., 2013; Sabia et al. 2015). The regions, where $\Lambda_p > 0$, indicate the potentially invasible habitats with respect to temperature, and the regions, where $\Lambda_p < 0$, are those non-invasible. The greater is the Λ_p, the higher is the yearly (periodic) fitness, or the potential invasibility (Fig. [6]). References of labels are as same as in Fig. 6.

data. The high R^2 and gradient close to 1 suggest that the difference between the two metrics is negligible. Thus, simplifying both Λ_p assuming V=0 from Eq. (3) is empirically reasonable approximation for *P. marinus*.

Furthermore, we compared Λ_p, computed via R_p (for V=0) from Eq. (4), denoted by $\Lambda_p(R_p)$, statistically, with Λ_p (for V≠0), to test the assumption $\xi(d) \approx 1$ in the derivation of R_p (see Eq. [D2] in Appendix [D]). We also computed the differences between the estimates of the metrics for the same temperature-time profiles. (Fig. 3C) shows the differences (in Ci) and the correlation (in Cii) between Λ_p from Eq. (3) for V≠0, and Λ_p computed via R_p (Eq. [4]) for V=0, for the same SST data. The high R^2 and gradient close to 1 suggest that the difference between the two metrics is negligible, especially where Λ_p is close to zero. Thus, the averaging of stage-based removal times, that is, the

assumption $\xi(d) \approx 1$ (in Eq. D2 in Appendix [D]) in the derivation of R_P, is a reasonable approximation for *P. marinus*. The assumption that $\xi(d) \approx 1$, together with V=0, therefore, suggests that R_P computed from Eq. (4) for V=0 is a reasonable approximation to evaluate and interpret the persistence and the growth of a population of *P. marinus*.

3.3. Predicted geographic distribution of P.marinus

We mapped out the *potentially invasible* marine habitats, i.e., isolating the temperature-time profiles, in Fig. 4, assuming other conditions, which are unknown, are suitable for *P. marinus,* at $1^0 \times 1^0$ resolution SST data given at long-term monthly means from NOAA-ESRL (n.d.), on the basis of Λ_p (Eq. [3]). We located the occurrences of *P. marinus* from the literature. The species occurrences detected, indicate that the direction of spread of *P. marinus* on a global scale is generally from native habitats with low Λ_p to colonized habitats with high Λ_p, consistent with the model prediction.

3.4. Approximation of periodic ambient temperature

Firstly, we tested how well long-term monthly mean SST data of $1^0 \times 1^0$ marine plots fit to a sinusoidal function $T_j = B_0 + B_1 \sin(2\pi t/t_p + B_2)$, for j=1,..,12 with period t_P=12 months, by minimizing the sum of squared residuals using *fminsearch* function in Matlab, to investigate the effect of the amplitude of temperature-time profiles on *periodic* fitness. Here, $B_0 B_1$ and B_2 are the average, amplitude and phase-shift of temperature, respectively. The goodness-of-fit, R^2, given for the data of each $1^0 \times 1^0$ marine plot from NOAA-ESRL (n.d.), averaged over each latitude (+90 – northern, to −90 – southern), is given in (Fig. 5A). The high R^2 were yielded for sub-tropical and temperate latitudes, indicating that sinusoidal function gives a good approximation to the long-term monthly mean SST data over yearly periods, where amplitudes are large, for generalization. Estimations of low R^2 at low- and high-latitude regions are due to small fluctuations of monthly mean temperatures around the yearly average that fail to form distinct sinusoidal patterns. Thus, both in cold-water seas, where periods are time-asymmetric, and tropical seas, the amplitudes are negligible.

We compared Λ_p (Eq. (3)), given by long-term monthly mean temperatures of 100 randomly selected $1^0 \times 1^0$ resolution marine plots, statistically, with Λ_p given by the sinusoidal functions fitted to the same data (Fig. (5B)). The high R^2 and gradient close to 1.0 suggest that difference between Λ_P, computed by monthly mean SST, and that computed via sinusoidal functions fitted to the same monthly data, is negligible. Thus, examining the effect of temperature-time profiles of habitats, in terms of means and amplitudes of sinusoidal functions with a period of year, on colonization dynamics, is a reasonable generalization to understand the full system.

3.5. Effect of amplitude on fitness

As the sinusoidal approximation is a good fit to monthly temperature data, to test the effect of amplitude of temperature on periodic fitness, we simulated Λ_p and R_p, both, with respect to a range of B_0 and B_1 of temperature-time profiles, using sinusoidal functions. Here, we set B_2=0 as phase-shift has no weight on the metric by theory. (Fig. 6A) shows the *periodic* fitness simulated for different means and amplitudes of habitat temperatures, using the sinusoidal function of monthly mean temperatures, with a period of year, with the approximation that fluctuations are symmetric, and where asymmetric, the amplitudes are negligible (as in (Fig. 5A)). The larger the amplitude, the lower is the *periodic* fitness of *P. marinus* for a given yearly mean temperature. An increase in the amplitude narrows-down the range of mean habitat temperatures that the species can persist. The native habitat range of the species is generally at high-amplitude temperature regions, resulting in low-fitness, compared to their colonized habitat range, which is generally at low-amplitude temperature regions, yielding greater fitness, within a finite range of yearly mean temperatures (Fig. (6B)).

3.6. Locality-specific population dynamics

(Fig. 7A) shows the sinusoidal temperature-time profile at Fukuyama harbor, modeled on the basis of the data from Kasahara et al. (1975). (Fig. 7B) shows the related cyclic growth dynamics of a *P. marinus* population, with an introduction of a single female, predicted by the calibrated model (Eq. (1)). The associated eigenvalues (real part) of stage-classes are shown in (Fig. 7C), and the stage-abundances are shown in (Fig. 7D). Here, we simulated the population dynamics at day's scale, assuming that each month has 30 days. We noted that the dominant stage-class was the naupli, in general, and the naupli stage IV in particular. The peak population abundance (in Fig. (7B)), and the dominant stages (in Fig. (7D)) are good qualitative matches compared with the data shown in Liang and Uye (1997a) for *P. marinus* at the same harbor.

4. Conclusions

Our study suggests that, the larger the amplitude of periodic (yearly) fluctuations of monthly (or seasonal) temperatures, or the yearly temperature cycles, the lower is the fitness, or the yearly (periodic) intrinsic growth rates, of *P. marinus* populations, vice versa, given that yearly mean temperatures and other environmental and

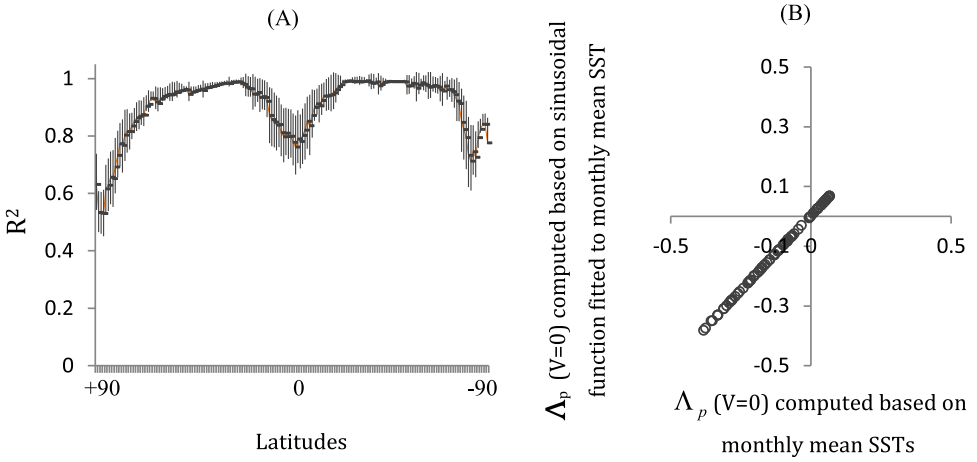

Fig. 5. (A) Goodness-of-fit R^2, averaged by latitude, for the sinusoidal functions fitted to long-term monthly mean sea surface temperature (SST) data of each $1^0 \times 1^0$ marine plot from NOAA-ESRL (n.d.). Bars represent the standard deviations. (B) Regression of Λ_p (V=0) from Eq. (3), computed based on long-term monthly mean SST data, vs. Λ_p (V=0), computed based on the fitted sinusoidal functions to the same data; for 100 randomly selected $1^0 \times 1^0$ marine plots. Regression yielded R^2=0.99 and gradient=1.0.

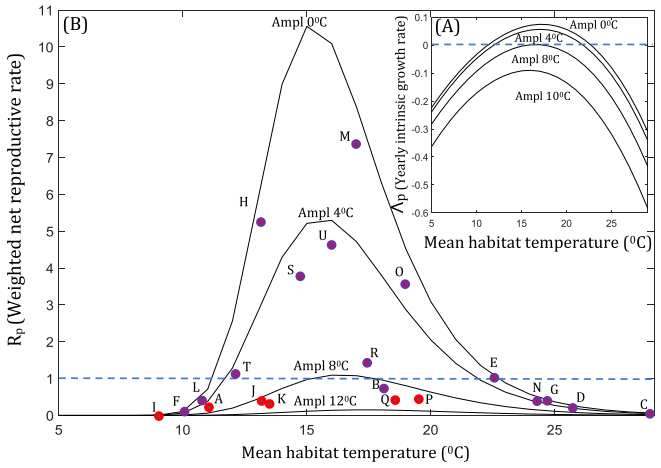

Fig. 6. (A) Yearly intrinsic growth rate Λ_p of *P. marinus* simulated for ranges of mean and amplitude of habitat temperatures on the basis of temperature-time sinusoidal functions. (B) Weighted net reproductive rate R_p of *P marinus* simulated with respect to the same mean and amplitudes of temperature-time profiles. Non-autonomous (i.e., amplitude >0) solutions of both Λ_p and R_p converge to autonomous (i.e., amplitude=0) solutions when amplitude tends to zero. Red circles show the native habitats surrounding the Sea of Japan (Walter, 1986), and purple circles show the habitats where *P. marinus* was detected (Olazabal and Tirelli, 2011; Brylinski et al., 2012; Jha et al., 2013; Sabia et al. 2015). Here, $R_p > 1$ and $\Lambda_p > 0$ are the range potentially invasible (or colonizable) to *P. marinus,* and $R_p < 1$ and $\Lambda_p < 0$ are the range non-invasible. The larger is the amplitude, the lesser is the periodic fitness, and the narrower is the range of mean temperatures of habitats invasible. [References: see Rajakaruna et al. (2012): (A) West coast of Hokkaido, Japan, Sato (1913), Sato Anraku (1953), Walter (1986b); (B) Yellow sea & East China sea, Qing-Chao and Shu-Zhen (1965); (C) Andaman Islands (Pillai, 1980); (D) Mauritius (Grindley and Grice, 1969); (E) Moreton Bay, Queensland (Greenwood, 1977); (F) Patagonian Waters, Southern Chile (Jones, 1966; Grindley and Grice, 1969) from Hirakawa (1986); (G) Oahu, Hawaii (Jones, 1966) (Carlton, 1985); (H) San Francisco Bay, California (Ruiz et al., 2000); (I) Peter the Great Bay (Brodsky, 1948, 1950); (J) Korea sea (Chiba, 1956; Tanaka, 1966, Tanaka and Huee, 1966), Walter, 1986b); (K) Korea sea, Brodsky (1948, 1950); (L) Elliot Bay, Puget Sound, Washington (Cohen, 2004), USGS; (M) San Diego Bay (USGS); (N) Off-Taiwan (Shen and Lee, 1963). (O) Todos Santos bay, Baja Cal (Jimenez-Perez and Castro-Longoria, 2006); (P) Tokyo bay (Tachibana et al., 2013); (Q) Chikugo river estuary (Suzuki et al., 2011); (R) Adriatic sea-Italy (Olazabal and Tirelli, 2011); (S) Lake Faro-North eastern Sicily (Sabia et al., 2012); (T) Gironde estuary, France (Jha et al., 2013); (U) Bay of Biscay, France (Brylinski et al., 2013).] Locality specific temperature-time data profiles are from the literature cited, or where not, from ESRL-NOAA (n.d.). [Temperature (mean, 2x amplitude): NOAA-ESRL: (A) 10.92,16.65; (B) 180.15, 17.8; (C) 28.63, 2.16; (D) 25,88, 4.39; (E) 22.40, 5.5; (F) 10.02, 3.80; (G) 24.52, 3.9; (H) 12.74,2.69; (I) 9.08, 7.5; (J, K) 12.95, 17.14 (L) 10.71, 6.59;(M) 17.05,5.32; (N) 24.58, 8.28; (O) 180.64,7.28 (Jimenez-Perez and Castro-Longoria, 2006); (P)180.75,20.03 (Tachibana et al., 2013); (Q) 180.5, 21.00 (Suzuki et al., 2012); (R) 17.32, 15.39 (Olazabal and Tirelli, 2011); (S) 14.72, 11.56 (Sabia et al., 2012); (T) 12,28, 9.42 (Jha et al., 2013); (U) 15,89,9.53 (Brylinski et al., 2013).].

ecological factors are constant. Thus, *P. marinus* populations migrating from habitats with high amplitude temperatures to that with low amplitudes, having similar other conditions, can potentially increase their yearly (periodic) fitness, substantially, exploiting the existing temperature amplitude gradient, and increasing their colonization potential. We showed that the process, by which this is mechanized, is that populations migrating from high- to low-amplitude yearly fluctuations will potentially produce greater number of offspring at the end of the periodic cycle through generations of females of an ovigerous female at the beginning of the periodic cycle. For this theory to be valid, we showed that the average stage-removal times (by maturation and mortality) have to be less than the lengths of time that a population stays in the given changes of temperature in discretized time-intervals. Hence, the impact of the amplitude of yearly temperature on fitness, which we theorize here, can be generally true for fast-maturing calanoid copepods, having shorter generation times, and having dependencies of vital rates on temperature similar to that of *P. marinus*. A large volume of literature indicates that these structural and functional relationships are generalizable to calanoid copepods: stage-structure (Mauchline and Mauchline, 1998); mortality rates (Hirst and Kiørboe, 2002; Bunker and Hirst, 2004); generation times (Huntley and Lopez, 1992); Gaussian type fecundity rates (for e.g., Uye, 1981; Sullivan and McManus, 1986; Saiz et al., 1999; Halsband-Lenk et al., 2002; Gislason, 2005; Holste and Peck, 2006; Kang et al., 2011); generalizations of vital rates for ectotherms (Amarasekare and Savage, 2011). Hence, this suggests that this phenomena we observed pertaining to *P. marinus* may be generalizable to similar other copepods. The potential geographic distribution, predicted by our metrics, on the basis of fitness given by the habitat temperature-time profiles, matched the field evidence of the species' occurrences, in general. This may suggest that *P. marinus* colonized low amplitude periodic (yearly) temperature habitats, such as the west coasts of North America, migrating from high amplitude periodic temperature native habitats surrounding the Sea of Japan, within a range of optimal yearly mean temperatures.

Of course, the demonstrated species spread was regardless of the fact that other environmental and ecological factors, such as salinity, species interactions, available niches, resource (food) limitations, Allee effects and so on, also could further limit their fitness and spread in the potentially invasible geographic range predicted by our metrics, isolating habitat temperature-time profiles, and assuming fixed optimal conditions of other factors. As there are multiple attributes to errors in the estimations and approximations; vital rates, temperatures, scaling, averaging of variations, influence of other biological and environmental factors, confounding effects due to interactions, and so on; a bloated confidence interval of the predicted range and the fitness could be a result, whereas our data were not sufficient to compute those fully. However, the range, outside the potentially colonizable range predicted by our metrics, limits growth due to temperature-profile dependent dynamics alone, regardless of how favorable those habitats are to other growth-affecting factors.

Our result that high amplitude periodic temperature lowers the population fitness, or their colonization potential, is also consistent with the broad stochastic theory, which suggests that increased environmental fluctuations, commonly computed at high frequencies, increase the extinction probability of local populations, in general (Lande et al., 2003). Hence, the range of habitats that are tolerable to the species, especially those in the temperate regions, could be narrowed-down, when periodic fluctuations of temperature are also taken into account, compared to the tolerable range predicted by the mean habitat temperatures alone (as in Strasser et al. (2011), Amarasekare and Savage (2011) and Rajakaruna et al. (2012)). This also falls in line with the theoretical arguments behind Savage (2004), as we stated earlier. Furthermore, our dynamical results are also consistent with Amarasekare and Coutinho (2013), who have shown that seasonal temperature variation allows populations to converge to a stationary stage distribution.

Bacaër (2012) defined a net reproductive rate in a variable environment as the asymptotic ratio of the total births in two successive generations of the family tree. For theoretical interest, the persistence condition based on our R_p can be interpreted in many ways. In essence, R_p is a weighted net reproductive rate, which is a measure of the periodic reproductive rate of a population subject to periodic external forcing cycles. Metric R_p determines the system stability, and the growth of a population across the periodic temperature fluctuations, in a biologically meaningful way, capturing the system functionality and transitions at the level of sub-stages of a population by geometrically averaging the weighted R_0's at piecewise temperatures in discretized times over an entire period. However, if our interest is only the population stability condition for a given habitat temperature-time profile, then maximal Floquet exponent, calculated based on time-averaged population matrix over a period, may suffice to evaluate the periodic persistence (Ma and Ma, 2006; Wesley and Allen, 2009).

As epipelagic species are more vulnerable to be transported via

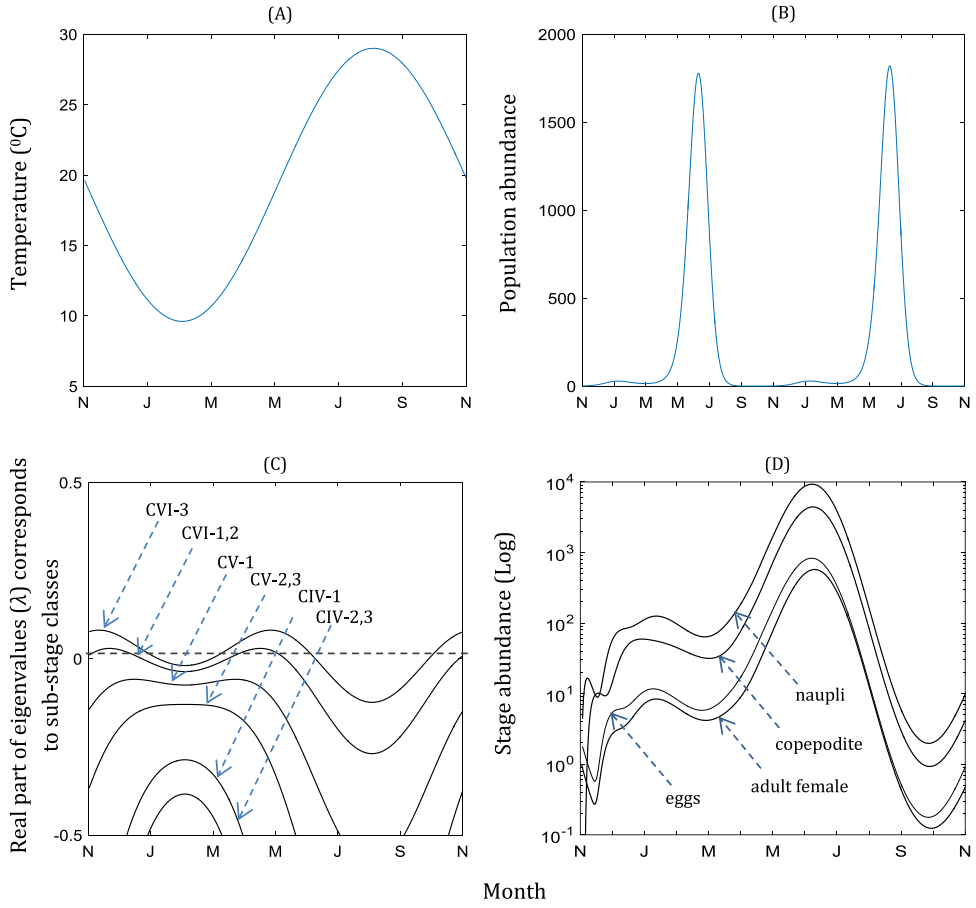

Fig. 7. Population dynamics of *P. marinus*, modeled with respect to temperature-time profile at Fukuyama harbor (Kasahara et al., 1975; Uye et al. 1982), starting with a single female at the beginning of November, simulated at day's scale, assuming each month has 30 days, based on the calibrated model Eq.(1). Here, for e.g., CVI-1,2 are the sub-stages 1 and 2 of copepodite stage CVI (the adult female stage). The dominant eigenvalue corresponds to the female-adult sub-stage CVI-3. The dominant stage-class becomes the naupli once the population reached a stable-stage distribution in periodically (yearly) changing temperatures. This theoretical result closely matches the dynamics observed for *P. marinus* in Liang and Uye (1997a) at the same harbor. Panel (D) and (Fig. 2C) may suggest that the daily rate of maturation (transition) of eggs into naupli is substantially faster than the rate of the production of eggs and the rate of maturation of naupli into copepodite.

ballast water, and be discharged into new habitats, there is a possibility that gradient in the degree of amplitudes among habitats in a region can play a major role in colonization and invasion of such fast-maturing species transported via ship ballast water. Thus, our theory may suggest that northern temperate marine ecoregions, such as, the Seas of Japan, China, Black, Caspian and Mediterranean, and Virginian, and so on, where the amplitudes of periodic (yearly) temperature are comparatively large (NOAA-ESRL), can be potential sources of copepods, and similar species, becoming invasive in potential sinks at low-amplitude temperature, in temperate regions, such as, the west coast of North America and the east coast of North Atlantic and so on, which are in close physical proximity, and also within a narrow range of yearly mean temperatures. Yet, of course the other factors can also vary drastically across these regions, both enhancing and lowering the temperature-amplitude-dependent advantage of the colonizing copepod species. However, supporting the temperature-amplitude-driven invasiveness proposition, we find evidence that eight invasive copepod species native to the coast of Japan have invaded San Francisco Bay and adjacent west coast of North America (Cordell et al., 2008), which have a steep amplitude gradient, high to low from the former to the latter, while their yearly average temperatures are similar. These species include two species of the same genus of *P. marinus*, namely, *P. inopinus* and *P. forbesi*. In contrast, there are no reports to date, which indicate that copepods native to the west coast of North America invaded the Sea of Japan or adjacent seas. In due course, invasive *P. inopinus* has become the dominant species at Columbia River estuary (Cordell et al., 1992), whereas *P. forbesi* has replaced some of the native species in the new habitats (Bollens et al., 2012) demonstrating their colonization potential.

We investigated the effect of yearly fluctuations of monthly mean temperatures on the stability and the growth of *P. marinus* populations, assuming that their stage-based vital rates, such as, fecundity, maturation and mortality, respond quantitatively to changes in monthly mean temperatures, but for smaller time-scales or instantaneous fluctuations. Yet, high frequency fluctuations (e.g., within a month) can have a dampening effect on the trends in fitness that we have observed at low frequencies (at monthly scale). As our estimations of vital rate parameters, modeled as functions of temperature, were made based on the data from experiments conducted at constant (or fixed levels of) temperatures over time, we may need to test the exact scales at which those parameters, and also growth rates, in general, respond quantitatively to the changes in temperature, to understand the full system.

Furthermore, calanoid copepods generally colonize the top water column (Bradford-Grieve, 2002). It has also been known that some copepod species migrate vertically on a diurnal basis, while some others maintain a vertical zonation. For species migrating to lower depths diurnally, the metabolically active zone can still be the near-surface layer: about 5.4% of their energy is expended while they are at lower depths (Calanus euxinus, Svetlichny et al., 2000). This suggests that, for such species, it may be the near-surface temperatures that affect more on the day-to-day metabolism. However, we used SST data, which generally represent the top 10 m of the sea or less, for predicting the potential geographic distribution of *P. marinus*. If diurnal vertical

migration results in daily exposure of individuals to waters at different temperatures, creating an effect similar to experiencing high frequency temperature fluctuations, then incorporating these variations can reduce the effect of yearly amplitude of temperature that we demonstrated here on the stability and the growth of a population.

If the amplitudes of periodic (yearly) SST fluctuations increase along with the gradual sea warming (see Masson and Cummins (2007)); as it can be observed in Race Rocks data, slightly (DFO Canada); our theory suggests that we could expect those to suppress the effect of increased mean habitat temperatures on the range expansion of the species. Thus, studying the changes in the whole temperature-time profile over time, at appropriate temporal and spatial scales, may be crucial when calibrating the effect of global warming on species range expansion, as they can create differential effects on population stability, counteracting the positive forces created on them by the general rise in the mean SST. This hypothesis also agrees with the theory by Savage (2004).

An extension to this study is to investigate how different frequencies in temperature impact the fitness.

Acknowledgements

Authors thank the Canadian Aquatic and Invasive Species Network (NSERC) (HR and ML), University of Alberta and Mathematical Biology Unit of Okinawa Institute of Science and Technology Graduate University (OIST) of Japan (HR), NSERC Discovery and Accelerator grants (ML), and a Killam Research Fellowship (ML). Comments from anonymous reviewers helped improving the paper immensely, for which we are very grateful.

Appendix A. Life history diagram

see Fig. A1.

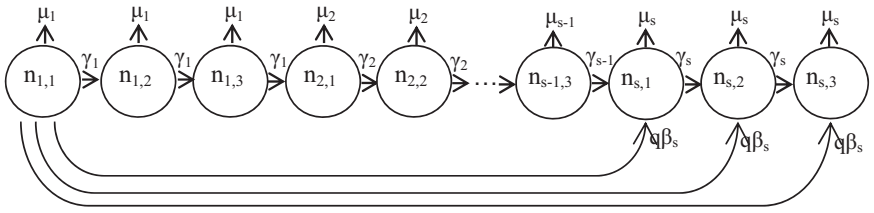

Fig. A1. Life history diagram of *P. marinus*. Here, μ_i are mortality rates, and γ_i are maturation rates of each 3 sub-stages of stage i. Furthermore, β_s is fecundity rate, and q is a constant, the proportion of ovigerous females in sub-stages of adult stage (s=12). Here, $n_{i,k}$ are the population abundance in each sub-stage k in stage i.

Appendix B. Matrix reduction

The system Eq. (1) is dynamically equivalent to a slightly simpler version, where the sub-stages of the last stage are lumped together, so that, the last two columns and rows are removed, and the remaining σ_s is replaced by μ_s. This is because the sub-stages of the last stage are functionally indistinguishable as there is no further transition of the population to another stage. Here, we drop the explicit dependence of parameters on T for notational simplicity. It yields, **A,** which has dimension lxl such that $l=k(s-1)+1$, and two sub-matrices: fecundity **F**, and transitions-mortality (removal) **L** , after partitioning **A**, such that **A=F-L** .

$$\mathbf{A}=\begin{pmatrix} -\sigma_1 & & & & \vdots & & q\beta \\ \gamma_1 & -\sigma_1 & & & \vdots & & \\ & \gamma_1 & -\sigma_1 & & \vdots & & \\ & & \gamma_1 & -\sigma_2 & \vdots & & \\ \vdots & \vdots & \vdots & \vdots & \vdots & \vdots & \vdots \\ & & & & \vdots & -\sigma_{s-1} & \\ & & & & \vdots & \gamma_{s-1} & -\mu_s \end{pmatrix} \mathbf{F}=\begin{pmatrix} & & & & \vdots & & q \\ & & & & \vdots & & \\ & & & & \vdots & & \\ & & & & \vdots & & \\ \vdots & \vdots & \vdots & \vdots & \vdots & \vdots & \vdots \\ & & & & & & \end{pmatrix} \mathbf{L}=\begin{pmatrix} \sigma_1 & & & & \vdots & & \\ -\gamma_1 & \sigma_1 & & & \vdots & & \\ & -\gamma_1 & \sigma_1 & & \vdots & & \\ & & -\gamma_1 & \sigma_2 & \vdots & & \\ \vdots & \vdots & \vdots & \vdots & \vdots & \vdots & \vdots \\ & & & & \vdots & \sigma_{s-1} & \\ & & & & \vdots & -\gamma_{s-1} & \mu_s \end{pmatrix}$$

Appendix C. Weighted net reproductive rate R_p

Here, we drop the explicit dependence of parameters on T for notational simplicity. If we consider temperature T to be constant, then the net reproductive rate R_0 is given by $\rho[\mathbf{FL}^{-1}]$, where ρ is the spectral radius of the next generation matrix $\mathbf{FL}^{-1}$ (Appendix [B]), that is, $\rho[\mathbf{FV}^{-1}]=\max_{1\le i\le n}|R_{0i}|$, where R_{01}, $R_{02}\ldots R_{0n}$ are the eigenvalues of the square matrix $\mathbf{FV}^{-1}$; the maximum real eigenvalue of the square matrix $\mathbf{FL}^{-1}$ (Rajakaruna et al., 2012). It yields

$$R_0=\frac{q\beta_s}{\mu_s}\prod_{i=1}^{s-1}\left(\frac{\gamma_i}{\gamma_i+\mu_i}\right)^k \tag{C1}$$

for a population in constant temperature T (Rajakaruna et al., 2012). We define $R_{0,j}$, λ_j and g_j to be the net reproductive rate, intrinsic growth rate, and mean sub-stage removal time, respectively, for temperature corresponding to time-interval j, for e.g., a month or a season, that is $(t_{jd}, t_{(j-1)d})$, associated with matrix $\mathbf{A_j}$ given for the interval j, where d is the number of days in the interval. From Eq. [D4] in Appendix [D], we can write the explicit functional relationship between $R_{O,j}$ and intrinsic growth rate λ_j at time interval j as

$$\lambda_j=\frac{1}{g_j}\left(R_{0,j}^{\left(\frac{1}{l}\right)}-1\right) \tag{C2}$$

We substitute $R_{0,j}$ from Eq. (C1) in Eq. (C2), and then λ_j from Eq. (C2) in $\Lambda_p = \bar{\lambda} + V$ (Eq. [3]), such that $\bar{\lambda} = \frac{1}{t_p}\sum_{j=1}^{m} \lambda_j (t_{jd} - t_{(j-1)d})$ and $V = \frac{1}{t_p}\sum_{j=1}^{m} \log(\mathbf{v}_{j-1}, \mathbf{v}_j)$, where t_p is the period, and $(\lambda_j, \mathbf{v}_j)$ is the dominant eigenpair of $\mathbf{A}_j$ for j=1..m, with eigenvector is normalized such that $(\mathbf{v}_j, \mathbf{v}_j)$ =1. It yields $\Lambda_p = \frac{1}{t_p}\sum_{j=1}^{m}\left(R_{0,j}^{\left(\frac{1}{l}\right)} - 1\right)\left(\frac{t_{jd} - t_{(j-1)d}}{g_j}\right) + V$ for habitat temperatures discretized into m piece-wise constant temperature intervals over the period. This can also be written as $\Lambda_p = \frac{G}{t_p}\left(\sum_{j=1}^{m} P_j R_{0,j}^{\left(\frac{1}{l}\right)} - 1\right) + V$. Here, $P_j = \left(\frac{t_{jd} - t_{(j-1)d}}{g_j}\right) / \sum_{j=1}^{m}\left(\frac{t_{jd} - t_{(j-1)d}}{g_j}\right)$ is the proportion of the number of sub-stages removed within the interval $(t_{jd}, t_{(j-1)d})$ at constant (or mean) temperature T_j, to the total number of sub-stages removed, G, within the period, that is,$G = \sum_{j=1}^{m}\left(\frac{t_{jd} - t_{(j-1)d}}{g_j}\right)$. Note that t_p/G is the average sub-stage removal time of the population within the period, which, we denote by g_P. This yields

$$\Lambda_p = \frac{1}{g_p}\left(\sum_{j=1}^{m} P_j R_{0,j}^{\left(\frac{1}{l}\right)} - 1\right) + V \tag{C3}$$

Thus, we define a *weighted net reproductive rate* as

$$R_p = \left(\sum_{j=1}^{m} P_j R_{0,j}^{\left(\frac{1}{l}\right)} + g_p V\right)^l \tag{C4}$$

such that Eq. (C3) can be written as,

$$\Lambda_p = \frac{1}{g_p}\left(R_p^{\frac{1}{l}} - 1\right) \tag{C5}$$

Note that Eq. (D4) in Appendix (D) is a special case of Eq. (C5) for the case when temperature is constant throughout the period. When V=0, $R_P = \left(\sum_{j=1}^{m} P_j R_{0,j}^{\left(\frac{1}{l}\right)}\right)^l$ in Eq. (C4). That is, when V=0, the weighted cumulative effect of $R_{0,j}^{\left(\frac{1}{l}\right)}$ of the discretized states becomes a good approximation to the final outcome of the system.

As the relationship between R_0 and λ (Eq. D4) is nested within the relationship R_P and Λ_p (Eq. C5) (for V=0), we expect Λ_p to be left-skewed compared to R_P for fixed amplitudes of temperature (see Fig. (6)). This is because $1/g_p$ is a positive exponential function of temperature similar to $1/g$ while R_P is generally a concave function of temperature similar to R_0. The R_0 and λ peak at different temperatures, with former always on the left of the latter. This has been observed in empirical data of many taxa by Huey and Berrigan (2001).

Appendix D. Explicit functional relationship between R_0 and λ

The intrinsic growth rate of a population, which is the dominant eigenvalue given by the system Eq. (1), for population in constant temperature environment, can be derived as a Lotka-Euler type equation solving the condition $\det[(\mathbf{F} - \mathbf{L}) - \mathbf{I}\lambda] = 0$, where $\mathbf{I}$ is the identity matrix, and λ are the eigenvalues of the matrix **F-L** (Appendix [B]). One way to do this is to transform **F-L** into a triangular matrix using Gaussian elimination method, and take the product of all the diagonal elements. It yields the following characteristic polynomial for λ,

$$1 = \frac{q\beta_s}{(\mu_s + \lambda)}\prod_{i=1}^{s-1}\left(\frac{\gamma_i}{\gamma_i + \mu_i + \lambda}\right)^k. \tag{D1}$$

Because matrix **A** has a Lefkovitch form, we know that the spectral bound of **A** is the dominant eigenvalue (that is the one with the largest spectral radius), and therefore, it is a real eigenvalue. This dominant eigenvalue is one of the l solutions to Eq. (D1). However, this is the only one of our interest from an invasibility perspective. We use λ to denote the dominant eigenvalue, which is the intrinsic growth rate in the population at constant temperature.

Dividing Eq. (C1) by Eq. (D1) and some manipulations yield a non-linear relationship between the net reproductive rate R_0 and the dominant eigenvalue λ, as $R_0 = \left(\frac{\mu_s + \lambda}{\mu_s}\right)\prod_{i=1}^{s-1}\left(\frac{\gamma_i + \mu_i + \lambda}{\gamma_i + \mu_i}\right)^k$. Recalling that $\sigma_i = \gamma_i + \mu_i$ is the overall removal rate in sub-stages in stage i, and $\sigma_s = \mu_s$ is the removal rate in the last sub-stage k of the stage i=s, we simplify the above equation as $R_0 = (1 + g_s\lambda)\prod_{i=1}^{s-1}(1 + g_i\lambda)^k$. Here, $g_i = 1/\sigma_i$ is the sub-stage removal time in stage i after maturation and mortality rates are combined together.

We assume identical sub-stage removal times for *P. marinus*, and will test this assumption later. Near-isochronal development is shown in many copepods at food saturation condition (Breteler et al., 1994), that is (g_i=g for i=1..s). This gives,$R_0 = (1 + g\lambda)^l$, where, $l = k(s - 1) + 1$. Choosing $g = \frac{1}{l}(g_s + k\sum_{i=1}^{s-1} g_i)$ to be the mean sub-stage removal time, and h_i=g_i-g to be the deviations from the mean, such that, $h_s + k\sum_{i=1}^{s-1} h_i = 0$, yields $R_0 = ((1 + g\lambda) + h_s\lambda)\prod_{i=1}^{s-1}((1 + g\lambda) + h_i\lambda)^k$, and hence, it yields

$$R_0 = (1 + g\lambda)^l \xi(h). \tag{D2}$$

Here, $\xi(h)$ is the error correction term given by $\xi(h) = \left(1 + \frac{h_s\lambda}{(1 + g\lambda)}\right)\prod_{i=1}^{s-1}\left(1 + \frac{h_i\lambda}{(1 + g\lambda)}\right)^k$. Taking the log transformation, and expanding it by Taylor series yields $\log \xi(h) = \left(\frac{\lambda}{(1 + g\lambda)}\right)(h_s + k\sum_{i=1}^{s-1} h_i) + \theta(h_i h_j)$ for $1 \le i, j \le s$. As $(h_s + k\sum_{i=1}^{s-1} h_i) = 0$, the above gives $\xi(h) \approx 1$ to the leading order in h_i (This has also been tested in the methods section.) Thus, using the approximation $\xi(h) \approx 1$, Eq. (D2) can be written as

$$R_0 = (1 + g\lambda)^l. \tag{D3}$$

Therefore, we can write Eq. (D3) as

$$\lambda = \frac{1}{g}\left(R_0^{\left(\frac{1}{l}\right)} - 1\right). \tag{D4}$$

This simple approximate relationship between λ and R_O is valid for populations in habitat temperatures T with negligible fluctuations. For special cases of this relationship, read Wallinga and Lipsitch (2007).

References

Amarasekare, P., Coutinho, R.M., 2013. The intrinsic growth rate as a predictor of population viability under climate warming. J. Anim. Ecol. 82 (6), 1240–1253.

Amarasekare, P., Savage, V., 2011. A framework for elucidating the temperature dependence of fitness. Am. Nat. 179 (2), 178–191.

Bacaër, N., 2012. On the biological interpretation of a definition for the parameter R0 in periodic population models. J. Math. Biol. 65 (4), 601–621.

Barone, S.R., Narcowich, M.A., F.J, 1977. Floquet theory and applications. Phys. Rev. A 15, 1109–1125.

Bollens, S.M., J.L. Breckenridge, J.R. Cordell, G. Rollwagen-Bollens, O. Kalata, R.C., Karatayev, A., 2012. Invasive copepods in the Lower Columbia River Estuary: seasonal abundance, co-occurrence and potential competition with native copepods. In: Proceedings of the 17th International Conference on Aquatic Invasive Species, Regional Euro-Asian Biological Invasions Centre (REABIC): San Diego, USA, September 2010. 7(1), 101–109.

Boltovskoy, D.A., Correa, N., 2011. Biological invasions: assessment of threat from ballast-water discharge in Patagonian (Argentina) ports. Environ. Sci. Policy 14 (5), 578–583.

Bradford-Grieve, J.M., 2002. Colonization of the pelagic realm by calanoid copepods. Hydrobiologia 485 (1–3), 223–244.

Breteler, W.C.M.K., Schogt, N., van der Meer, J., 1994. The duration of copepod life stages estimated from stage-frequency data. J. Plankton Res. 16 (8), 1039–1057.

Brylinski, J.M., Antajan, E., Raud, T., Vincent, D., 2012. First record of the Asian copepod *P. marinus* Sato, 1913 (Copepoda: Calanoida: Pseudodiaptomidae) in the southern bight of the North Sea along the coast of France. Aquat. Invasions 7 (4), 577–584.

Bunker, A.J., Hirst, A.G., 2004. Fecundity of marine planktonic copepods: global rates and patterns in relation to chlorophyll a, temperature and body weight. Mar. Ecol. Prog. Ser. 279, 161–181.

Cordell, J.R., Bollens, S.M., Draheim, R., Sytsma, M., 2008. Asian copepods on the move: recent invasions in the Columbia–Snake River system, USA. ICES J. Mar. Sci. 65 (5), 753–758.

Cordell, J.R., Lawrence, D.J., Ferm, N.C., Tear, L.M., Smith, S.S., Herwig, P.P., 2009. Factors influencing densities of non-indigenous species in the ballast water of ships arriving at ports in Puget Sound, Washington, United States. Aquat. Conserv.: Mar. Freshw. Ecosyst. 19 (3), 322–343.

Cordell, J.R., Morgan, C.A., Simenstad, C.A., 1992. Occurrence of the Asian calanoid copepod Pseudodiaptomus inopinus in the zooplankton of the Columbia River estuary. J. Crustace. Biol. 12 (2), 260–269.

Cox, D.R., 1967. Renewal Theory. Science Paperbacks and Methuen & Co. Ltd., GB, 142.

Damerau, M., Matschiner, M., Salzburger, W., Hanel, R., 2012. Comparative population genetics of seven notothenioid fish species reveals high levels of gene flow along ocean currents in the southern Scotia Arc, Antarctica. Polar Biol. 35 (7), 1073–1086.

DFO Canada. (n.d.). BC Lighthouse website. Retrieved from: ⟨http://www.pac.dfo-mpo.gc.ca/science/oceans/data-donnees/lighthouses-phares/index-eng.htm⟩.

Gislason, A., 2005. Seasonal and spatial variability in egg production and biomass of Calanus finmarchicus around Iceland. Mar. Ecol. Prog. Ser. 286, 177–192.

Gillespie, R.G., Baldwin, B.G., Waters, J.M., Fraser, C.I., Nikula, R., Roderick, G.K., 2012. Long-distance dispersal: a framework for hypothesis testing. Trends Ecol. Evol. 27 (1), 47–56.

Gillooly, J.F., Brown, J.H., West, G.B., Savage, V.M., Charnov, E.L., 2001. Effects of size and temperature on metabolic rate. Science 293 (5538), 2248–2251.

Gökçek, C., 2004. Stability analysis of periodically switched linear systems using Floquet theory. Math. Probl. Eng. 2004 (1), 1–10.

Halsband-Lenk, C., Hirche, H.J., Carlotti, F., 2002. Temperature impact on reproduction and development of congener copepod populations. J. Exp. Mar. Biol. Ecol. 271 (2), 121–153.

Hirst, A.G., Kiørboe, T., 2002. Mortality of marine planktonic copepods: global rates and patterns. Mar. Ecol.-Prog. Ser. 230, 195–209.

Holste, L., Peck, M.A., 2006. The effects of temperature and salinity on egg production and hatching success of Baltic Acartia tonsa (Copepoda: Calanoida): a laboratory investigation. Mar. Biol. 148 (5), 1061–1070.

Huey, R.B., Berrigan, D., 2001. Temperature, demography, and ectotherm fitness. Am. Nat. 158 (2), 204–210.

Huntley, M.E., Lopez, M.D., 1992. Temperature-dependent production of marine copepods: a global synthesis. Am. Nat., 201–242.

Hulme, P.E., 2009. Trade, transport and trouble: managing invasive species pathways in an era of globalization. J. Appl. Ecol. 46 (1), 10–18.

Jensen, J.L.W.V., 1906. Sur les fonctions convexes et les inégalités entre les valeurs moyennes. Acta Math. 30 (1), 175–193.

Jha, U., Jetter, A., Lindley, J.A., Postel, L., Wootton, M., 2013. Extension of distribution of Pseudodiaptomus marinus, an introduced copepod, in the North Sea. Mar. Biodivers. Rec. 6, e53.

Kang, H.K., Lee, C.R., Choi, K.H., 2011. Egg production rate of the copepod Calanus sinicus off the Korean coast of the Yellow Sea during spring. Ocean Sci. J. 46 (3), 133–143.

Kasahara, S., Uye, S., Onbé, T., 1975. Calanoid copepod eggs in sea-bottom muds. II. Seasonal cycles of abundance in the populations of several species of copepods and their eggs in the Inland sea of Japan. Mar. Biol. 31 (1), 25–29.

Kiørboe, T., Hirst, A.G., 2008. Optimal development time in pelagic copepods. Mar. Ecol. Prog. Ser. 367, 15–22.

Kiørboe, T., Sabatini, M., 1994. Reproductive and life cycle strategies in egg-carrying cyclopoid and free-spawning calanoid copepods. J. Plankton Res. 16 (10), 1353–1366.

Kiørboe, T., Sabatini, M., 1995. Scaling of fecundity, growth and development in marine planktonic copepods. Mar. Ecol. Prog. Ser. 120 (1-3), 285–298.

Klausmeier, C.A., 2008. Floquet theory: a useful tool for understanding non-equilibrium dynamics. Theor. Ecol. 1 (3), 153–161.

Lande, R., Engen, S., Saether, B.E., 2003. Stochastic Population Dynamics in Ecology And Conservation. Oxford University Press, Oxford, 212.

Lefkovitch, L.P., 1965. The study of population growth in organisms grouped by stages. Biometrics, 1–18.

Liang, D., Uye, S., 1997a. Population dynamics and production of the planktonic copepods in a eutrophic inlet of the Inland Sea of Japan. IV. *Pseudodiaptomus marinus*, the egg-carrying calanoid. Mar. Biol. 128 (3), 415–421.

Liang, D., Uye, S., 1997b. Seasonal reproductive biology of the egg-carrying calanoid copepod Pseudodiaptomus marinus in a eutrophic inlet of the Inland Sea of Japan. Mar. Biol. 128 (3), 409–414.

Lockwood, J.L., Hoopes, M.F., Marchetti, M.P., 2013. Invasion Ecology. John Wiley & Sons, 380.

Ma, J., Ma, Z., 2006. Epidemic threshold conditions for seasonally forced seir models. Math. Biosci. Eng. 3 (1), 161–172.

Mauchline, J., Mauchline, J., 1998. The Biology of Calanoid Copepods. Academic press, U.K, 710.

Masson, D., Cummins, P.F., 2007. Temperature trends and interannual variability in the Strait of Georgia, British Columbia. Cont. Shelf Res. 27 (5), 634–649.

Moler, C., van Loan, C., 2003. Nineteen dubious ways to compute the exponential of a matrix, twenty-five years later. SIAM Rev. 45 (1), 3–49.

NOAA-ESRL (n.d.). Physical Sciences Division, Boulder Colorado, USA. ⟨http://www.esrl.noaa.gov/psd/data/gridded/data.noaa.oisst.v2.html⟩ Data extracted in 2014.

Olazabal, A., Tirelli, V., 2011. First record of the egg-carrying calanoid copepod Pseudodiaptomus marinus in the Adriatic Sea. Mar. Biodivers. Rec. 4 (1), e85.

Rajakaruna, H., Strasser, C., Lewis, M., 2012. Identifying non-invasible habitats for marine copepods using temperature-dependent R0. Biol. Invasions 14 (3), 633–647.

Read, K.L.Q., Ashford, J.R., 1968. A system of models for the life cycle of a biological organism. Biometrika 55 (1), 211–221.

Ruiz, G., Fofonoff, P., Steves, B., Dahlstrom, A., 2011. Marine crustacean invasions in North America: A synthesis of historical records and documented impacts. In: In the Wrong Place-Alien Marine Crustaceans: Distribution, Biology and Impacts. Springer, Netherlands, 215–250.

Sabia, L., Zagami, G., Mazzocchi, M.G., Zambianchi, E., Uttieri, M., 2015. Spreading factors of a globally invading coastal copepod. Mediterr. Mar. Sci. 16 (2), 460–471.

Saiz, E., Calbet, A., Irigoien, X., Alcaraz, M., 1999. Copepod egg production in the western Mediterranean: response to food availability in oligotrophic environments. Mar. Ecol. Prog. Ser. 187, 179–189.

Savage, V.M., 2004. Improved approximations to scaling relationships for species, populations, and ecosystems across latitudinal and elevational gradients. J. Theor. Biol. 227 (4), 525–534.

Savage, V.M., Gillooly, J.F., Brown, J.H., West, G.B., Charnov, E.L., 2004. Effects of body size and temperature on population growth. Am. Nat. 163 (3), 429–441.

Strasser, C.A., Lewis, M.A., DiBacco, C., 2011. A mechanistic model for understanding invasions: using the environment as a predictor of population success. Divers. Distrib. 17 (6), 1210–1224.

Sullivan, B.K., McManus, L.T., 1986. Factors controlling seasonal succession of the copepods Acartia hudsonica and *A. tonsa* in Narragansett Bay, Rhode Island: temperature and resting egg production. Mar. Ecol. Prog. Ser. 28, 121–128.

Svetlichny, L.S., Hubareva, E.S., Erkan, F., Gucu, A.C., 2000. Physiological and behavioral aspects of Calanus euxinus females (Copepoda: calanoida) during vertical migration across temperature and oxygen gradients. Mar. Biol. 137 (5–6), 963–971.

Uye, S.I., 1981. Fecundity studies of neritic calanoid copepods Acartia clausi Giesbrecht and *A. Steueri* Smirnov: a simple empirical model of daily egg production. J. Exp. Mar. Biol. Ecol. 50 (2–3), 255–271.

Uye, S., Iwai, Y., Kasahara, S., 1982. Reproductive biology of Pseudodiaptomus marinus (Copepoda: Calanoida) in the inland sea of Japan. Bull. Plankton Soc. Jpn. 29, 25–35.
Uye, S., Iwai, Y., Kasahara, S., 1983. Growth and production of the inshore marine copepod Pseudodiaptomus marinus in the central part of the Inland Sea of Japan. Mar. Biol. 73 (1), 91–98.
Walter, T.C., 1986. New and poorly known Indo-Pacific species of Pseudodiaptomus (Copepoda: Calanoida), with a key to the species groups. J. Plankton Res. 8 (1), 129–168.
Wallinga, J., Lipsitch, M., 2007. How generation intervals shape the relationship between growth rates and reproductive numbers. Proc. R. Soc. B: Biol. Sci. 274 (1609), 599–604.
Wang, X., Hale, J.K., 2001. On monodromy matrix computation. Comput. Methods Appl. Mech. Eng. 190 (18), 2263–2275.
Wesley, C.L., Allen, L.J., 2009. The basic reproduction number in epidemic models with periodic demographics. J. Biol. Dyn. 3 (2–3), 116–129.